Hindawi Publishing Corporation
Advances in Tribology
Volume 2012, Article ID 723919, 12 pages
doi:10.1155/2012/723919

Research Article

Surface Layer Properties after Successive EDM or EDA and Then Superficial Roto-Peen Machining

Agnieszka Dmowska, Bogdan Nowicki, and Anna Podolak-Lejtas

Institute of Manufacturing Technology, Warsaw University of Technology, 02-524 Warsaw, Poland

Correspondence should be addressed to Bogdan Nowicki, bnow@meil.pw.edu.pl

Received 19 December 2011; Revised 3 April 2012; Accepted 3 April 2012

Academic Editor: J. Paulo Davim

The paper presents the results of the influence of basic electrical discharge machining EDM parameters and electrical discharge alloying EDA parameters on surface layer properties and on selected performance properties of machine parts after such machining but also the influence of superficial cold-work treatment applied after the EDM of EDA on modification of these properties. The investigations included texture of the surface, metallographic microstructure, microhardness distribution, fatigue strength, and resistance to abrasive wear. It was proved that the application of the roto-peen after the EDM and the EDA resulted in lowering roughness height up to 70%, the elevation of surface layer microhardness by 300–700 μHV, and wear resistance uplifting by 300%.

1. Basics of the EDM, the EDA, and the Roto-Peen Machining

Electrical discharge machining (EDM) is widely used in manufacturing of accurate parts of complex shapes, built of hard and impossible-to-cut or hard-to-cut materials [1, 2].

Electrical discharge alloying (EDA) is applied for generation of surface layer (SL) with volume share of up to several dozens percent of alloy elements. Such layers are up to 200 μm thick and they can be useful in wear-resistant tooling, erosion-resistant equipment, and so forth [3, 4].

The EDM and EDA processes are defined by spark discharge and the associated physical processes. Such processes take place in the presence of dielectric—in the EDM usually kerosene or water is employed and the spark discharges release energy of several millijoules while the EDA process is carried out in air, neutral gas, oil or kerosene, and the spark discharge energy is much higher and discharge duration is longer. Spark discharge generate much heat on small surface of the anode and the cathode. Power density inside the spark channel has been estimated as 10^{17} W/m^2 and local temperature could be raised up to 20 000 Kelvin degree [1, 3, 5, 6].

The eruption of molten material is critically important for material removal in the EDM process. Spark discharge results in local material loss, the craters and flashes are formed (Figure 1), and they are covered with the thin film of previously molten and then solidified metal [1, 7]. The volume of material removed from a single crater is $v = 1500 \div 3\,000\,000$ (μm^3).

Due to repeatedly occurring spark discharges, a surface layer of specific isotropic roughness is being created and this layer shows different metallographic microstructure and microhardness than that of the core. Tensile stress and microcracks are likely be present there in the case of the EDM carried out with medium or high energy of discharges [1, 5, 8, 9].

Two basic processes take place in the EDA and the associated mass transport can be observed as well. The first process consists in crater creation and mass loss on the cathode, while in the other one, mass transport, takes place through the spark channel and formation of highland in the crater (Figure 2), chemical composition of which is enriched by the alloying components [3, 4]. Surface layer (SL) created in the EDA process resembles the surface layer created in the EDM in view of similar phenomena

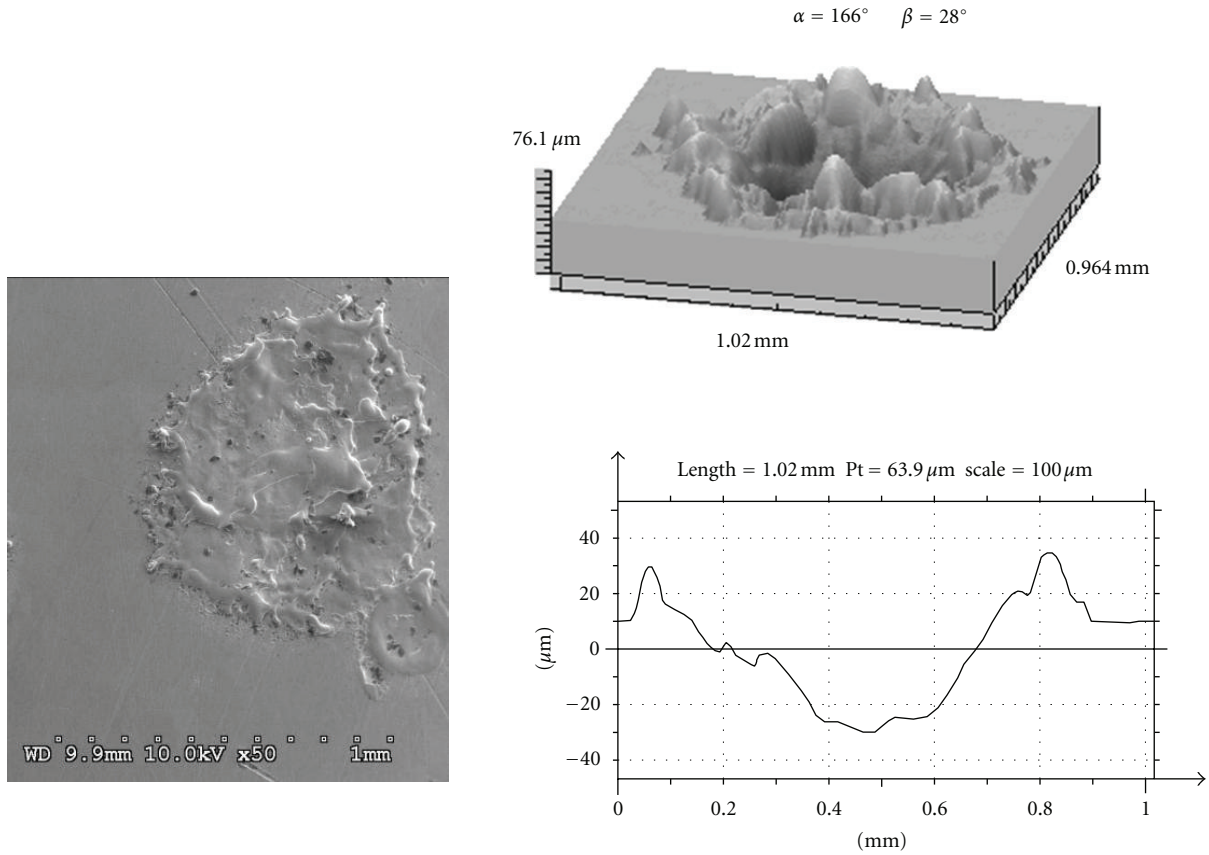

Figure 1: The SEM image of an individual electric discharge on the machined surface, its 3D view, and its profilogram (U = 80 V, I = 48 A, Ti = 400 μs).

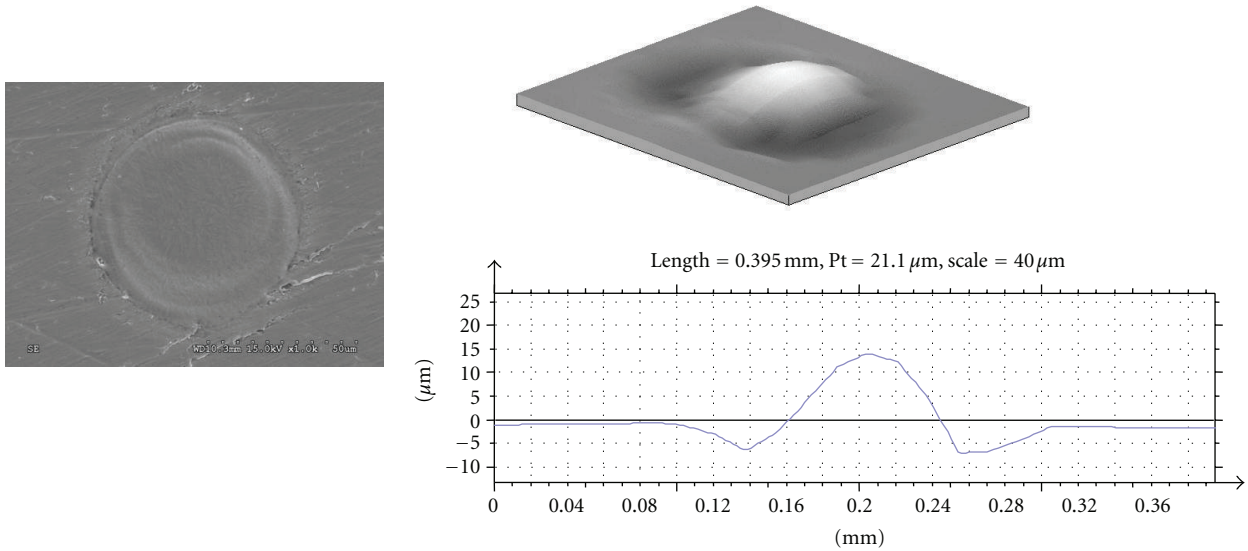

Figure 2: SEM image of individual discharge trace during the EDA on the machined surface, its 3D view and profilogram for U = 160 V, I = 8 A, Ti = 50 μs.

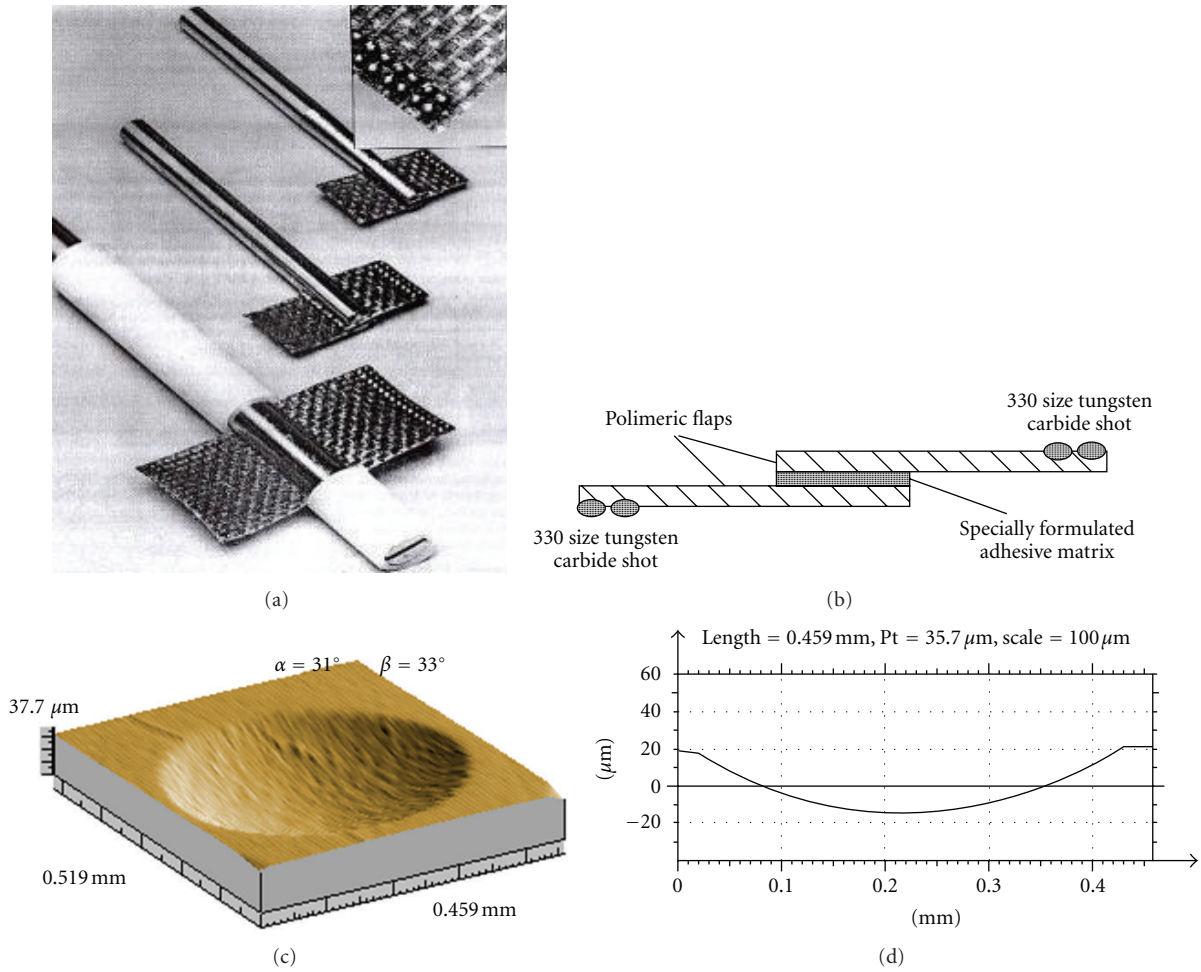

Figure 3: (a, b) Tools for the roto-peen machining; (c) view of a trace of a single ball hit; (d) its profilogram (Fn = 400 N; 34 HRC).

influencing the machining process with one exception—its chemical composition is different. These SL similarities include metallographic structure and microhardness which shows difference when compared to the core, the presence of tensile stress and microcrack occurrence.

When analyzing process of surface layer constitution, we can isolate three basic types of interaction: thermal phenomena, metallurgic phenomena, and mechanical phenomena.

In the EDM process, thermal and metallurgic phenomena prevail: melting, solidification, microstructural change and their results—change of structure, microhardness, stress, and microcracks.

In the EDA, phenomena resembling those present in the EDM occur but change of chemical composition takes place as well and is connected with spark discharge and with mass transport from the anode to the cathode.

Mechanical processes are typical of superficial cold-work treatment such as roto-peen (R-P) [10–13] and they can result in strain hardening of material (increase in SL hardness), introduction of compressive stress into the SL, elimination or reduction of microcracks which translates into elimination or minimization of adverse phenomena taking place during surface layer formation after the EDM and EDA process [14, 15].

The roto-peen machining process elaborated by the Boeing and 3M company [2, 9] consists in dynamic interaction between little balls of cemented carbide, 1 mm in diameter, fixed to the blades made of glass fiber balls (Figure 3) which rotate with the speed of revolution $n = 3\,000$–$8\,000$ rev/min. Because of the repeated balls against the machined surface, the elastic and plastic deformations follow in surface layer resulting in surface smoothing, superficial strain hardening, introduction of the compressive stress into the surface layer, and increase in fatigue resistance and resistance to abrasive wear. As the size of ball imprint d on the surface is known, one can determine the cold-work depth Z as well as the depth of residual stress existence, which is around 40–80% larger than cold work depth. These numbers should be greater than the depth of the surface layer generated in the EDM and EDA preceding the roto-peen machining.

The impact of a single roto-peen ball interaction on the cold-work depth can be determined (according to Drozd) based on the empirical relationship [10, 12]:

$$Z = 5.5h\frac{D}{d}, \tag{1}$$

Table 1: Specification of surface microstereometry (3D) after the EDM and then the roto-peen machining.

Parameters EDM			Parameters roto-peen		Microstereometric parameters 3D					
U (V)	I (A)	Ti (μs)	v (rev/min)	t (min)	S_a (μm)	S_t (μm)	S_p (μm)	S_{dq}	S_{sc} (1/μm)	ST_p (%)
120	24	200	—	—	12.40	87.2	47.5	0.40	0.10	0.80
120	24	200	5000	2.5	4.84	52.9	12.3	0.21	0.02	5.81
120	24	200	5000	5	2.04	27.3	14.2	0.08	0.01	0.00
120	24	200	7000	2.5	6.35	67.6	25.8	0.23	0.03	0.20
120	24	200	7000	5	3.37	41.7	14.6	0.12	0.02	0.30
80	48	400	—	—	13.30	149.0	92.6	0.4	0.03	0.2
80	48	400	5000	2.5	11.30	88.7	22.9	0.31	0.04	4.52
80	48	400	5000	5	6.23	50.4	17.6	0.20	0.03	1.73
80	48	400	7000	2.5	6.19	55	19.8	0.22	0.03	0.40
80	48	400	7000	5	6.51	57.8	17.4	0.16	0.02	3.26
160	16	800	—	—	8.91	78.8	35.4	0.26	0.06	0.60
160	16	800	5000	2.5	5.42	48.1	13.3	0.16	0.01	6.20
160	16	800	5000	5	5.19	47.2	12.8	0.16	0.01	9.55
160	16	800	7000	2.5	5.00	48.1	15.7	0.17	0.02	4.39
160	16	800	7000	5	3.78	53.7	16.4	0.16	0.03	0.60
160	6	100	—	—	4.47	47.4	16.5	0.27	0.01	0.50
160	6	100	5000	2.5	1.31	15.3	15.3	0.05	0.02	0.10
160	6	100	5000	5	1.14	28.5	28.5	0.06	0.02	0.00
160	6	100	5000	7.5	1.36	17	17	0.09	0.02	0.01
160	6	100	7000	2.5	1.66	35.5	35.5	0.08	0.02	0.00

where h: depth of the ball imprint, D: ball diameter, and d: diameter of a ball imprint on flat surface.

The research conducted in Warsaw University of Technology, Institute of Manufacturing Technology, was aimed at determining the effectiveness of superficial (roto-peen) cold-work treatment application for elimination of the adverse surface layer features being a consequence of the EDM and EDA.

The experimental investigation included evaluation of surface integrity after the EDM and EDA as well as after combined the EDM + cold work treatment and the EDA + superficial cold work treatment and it concerned the following areas: texture of surface, metallographic microstructure, microhardness distribution, residual stress distribution, fatigue resistance, and resistance to abrasive wear.

2. Results of Investigation for Surface Layer Properties and Selected Performance Features after the EDM and after Combined EDM + Roto-Peen Treatment

Research has been conducted for typical materials and typical conditions of machining. Samples made of hardened steel NC10 have been subjected to electrical discharge machining using a copper tool electrode mounted on the EDM center ROBOFROM 30 and the following parameters were selected: $U = 160$ V, $I = 6$ A, Ti = 100 μs, and $U = 160$ V, $I = 16$ A, Ti = 800 μs, which are typical of finishing machining, then the following parameters: $U = 120$ (V), $I = 24$ (A), Ti = 200 (μs), which are typical of semifinishing and then $U = 80$ V, $I = 48$ A, Ti = 400 μs, for the most productive machining type (Table 1).

Typical 3D views and profilograms of the EDM-ed and then roto-peened surfaces have been presented in Figures 4 and 5 for various parameters.

Microgeometry of the roughly EDM-ed and then roto-peened surfaces is typical of wide-spread and smooth summits and of microindents left as remnant of the EDM. Surface texture image in this case does not show much difference for all investigated parameter range. The level of height parameters gets less than one-third the initial value, for example, Ra drops from 21 μm to 6 μm and summit curvatures Ssc from 0.04 to 0.02 (1/μm). Machining time $t = 2.5$ (min) is needed for a complete smoothing of 10×20 surface at $n = 7000$ (rev/min); $t = 5$ (min) at $n = 5000$ (rev/min).

The investigation of surface layer was aimed at assessing the influence of the roto-peen machining on surface layer properties after consecutive EDM and roto-peen machining and particular attention was paid to possible presence of discontinuities, microcracks which can persist in surface layer after the EDM; microhardness distribution were obtained and surface uniformity was assessed.

Figure 6 shows images taken as microscopy view of polished sections for specimens machined by the EDM and the roto-peen. Surface layer obtained in the EDM features considerable nonuniformity and microcracks.

Analysis of the examination for surface layer microstructure and its thickness after the EDM and the roto-peen machining showed that surface layer is uniform and deprived of any visible micro-cracks or discontinuities in all cases.

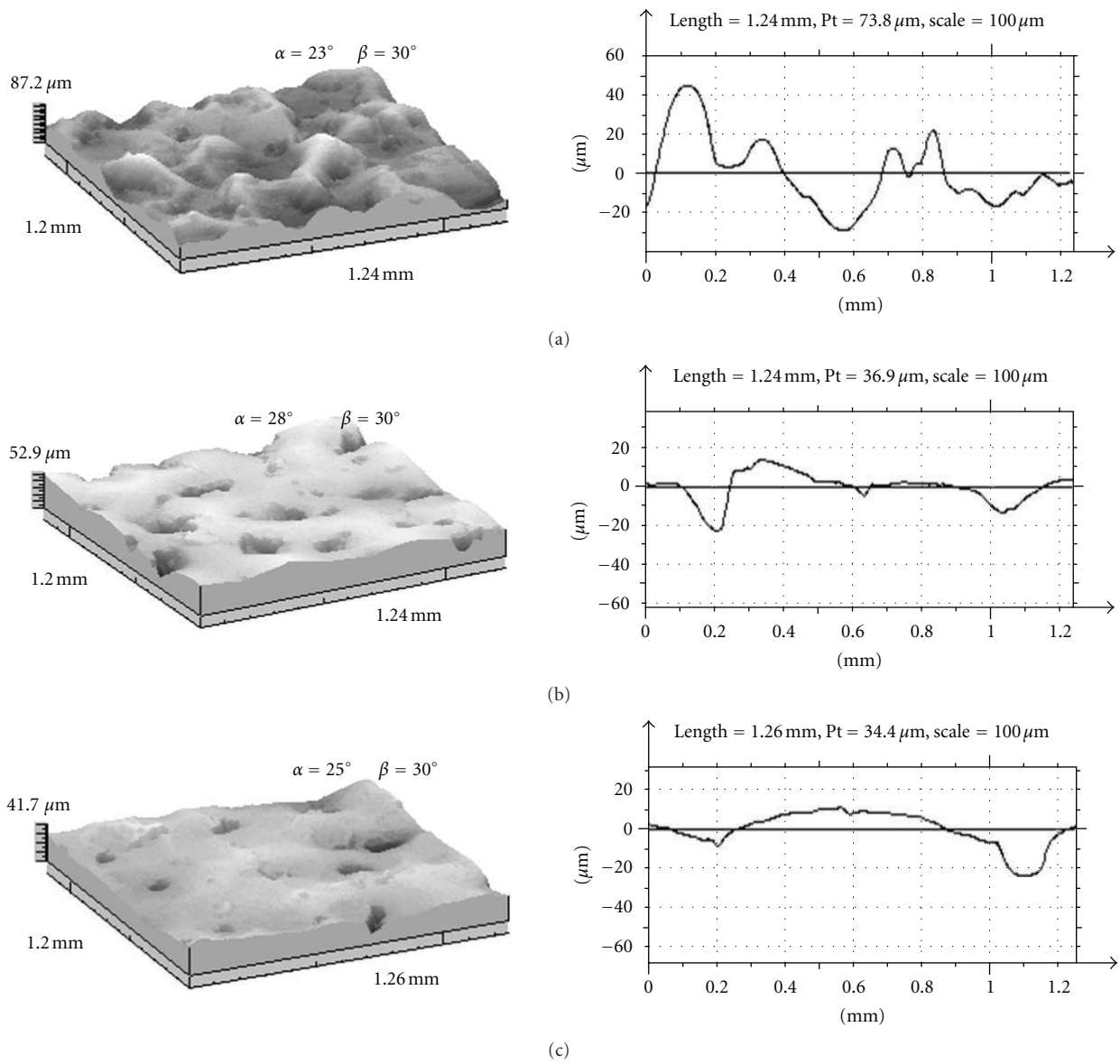

Figure 4: Stereometric image of surface after machining and its profilogram (a) the EDM—$U = 120$ (V), $I = 24$ (A), Ti = 200 (μs), and the following roto-peen (b) $n = 6500$ (rev/min), $t = 2.5$ (min), (c) $n = 6500$ (rev/min), $t = 5$ (min).

Surface layer thickness after two consecutive machining runs is much more uniform than after a single-EDM machining.

Microhardness examination has been conducted for the EDM-ed as well as EDM-ed and then roto-peened specimens and the following machining parameters have been applied:

(i) $n_1 = 5000$ obr/min, $t_1 = 2.5$ min, $t_2 = 5$ min,

(ii) $n_2 = 7000$ obr/min, $t_1 = 2.5$ min, $t_2 = 5$ min.

Typical micro-hardness distribution of surface layer after the EDM (Figure 7(a)) and the roto-peen applied after the EDM has been presented on Figure 7(b).

Analysis of microhardness distribution of the in-depth surface layer showed that application of the roto-peen machining which follows the EDM results in considerable micro-hardness SL increase from ca. 800 μHV up to 1100 μHV and surface layer improvement as to microgeometry, metallographic structure, and microcrack occurrence.

The residual stress investigations after the EDM and combined EDM + roto-peen machining have shown that after the EDM, the tensile stress taking values up to $s = +650$ MPa occurs and the application of the roto-peen after the EDM causes shift of this stress into compressive stress taking values up to $s = -1200$ MPa.

The scope of experimental investigation covered two basic performance properties, that is, resistance to abrasive wear and fatigue strength. The experiments of resistance to wear have been performed on Skoda-Savin machine. The assessment of resistance to wear consists in measuring the volume of an indent created on the surface of the examined

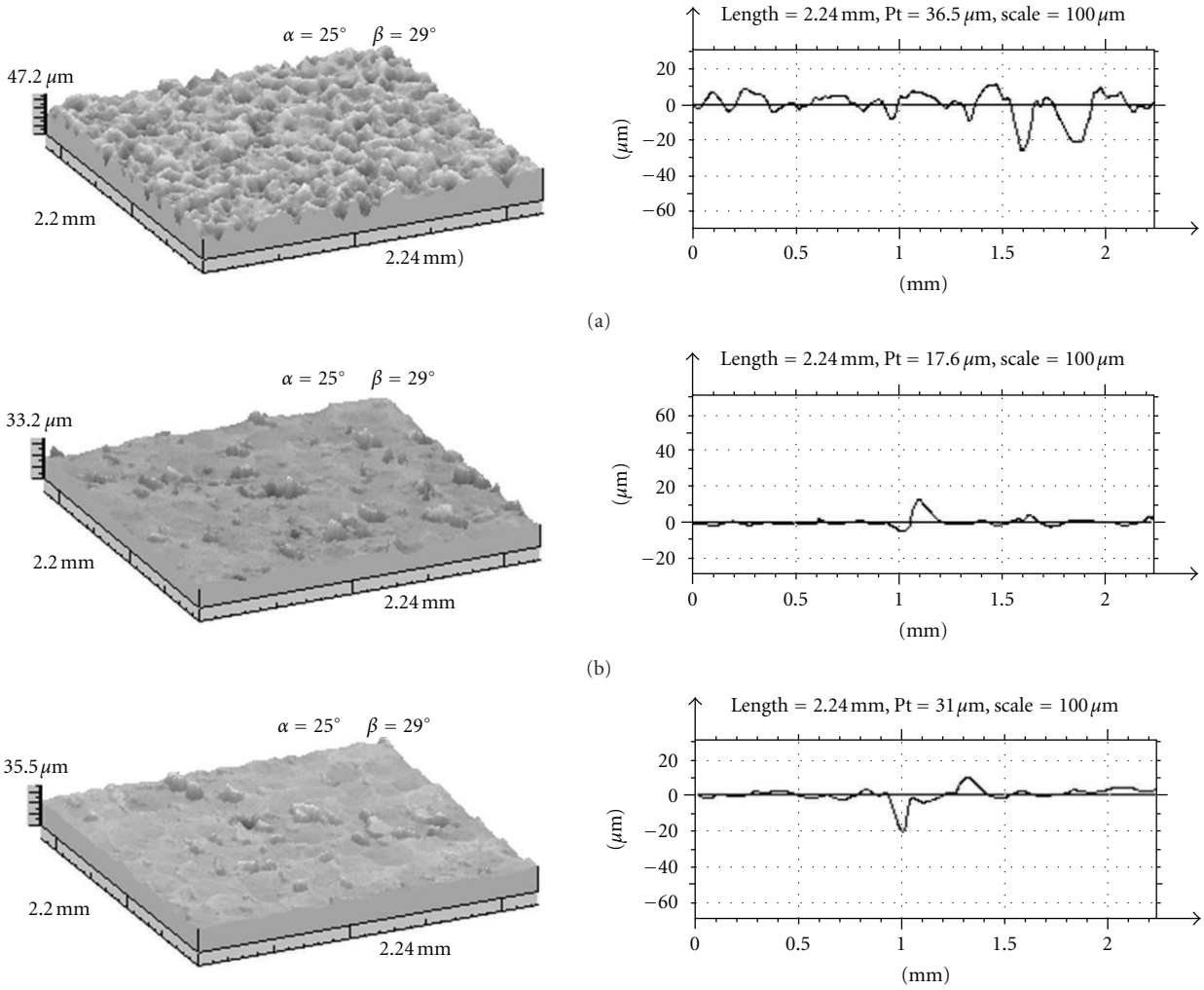

Figure 5: Stereometric image of surface after machining and its profilogram (a) the EDM– $U = 160$ (V), $I = 6$ (A), Ti = 100 (μs), and the following roto-peen (b) $n = 6500$ (rev/min), $t = 2.5$ (min), (c) $n = 6500$ (rev/min), $t = 5$ (min).

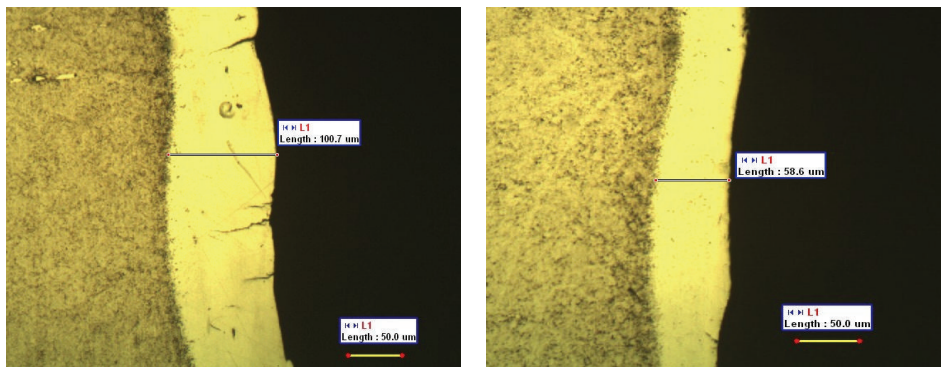

(a) (b)

Figure 6: Surface layer microstructure after the: (a) EDM $U = 80$ (V), $I = 48$ (A), Ti = 400 (μs), (b) EDM $U = 80$ (V), $I = 48$ (A), Ti = 400 (μs), Tp = 50 (μs) and roto-peen $n = 5000$ (rev/min), $t = 5$ (min).

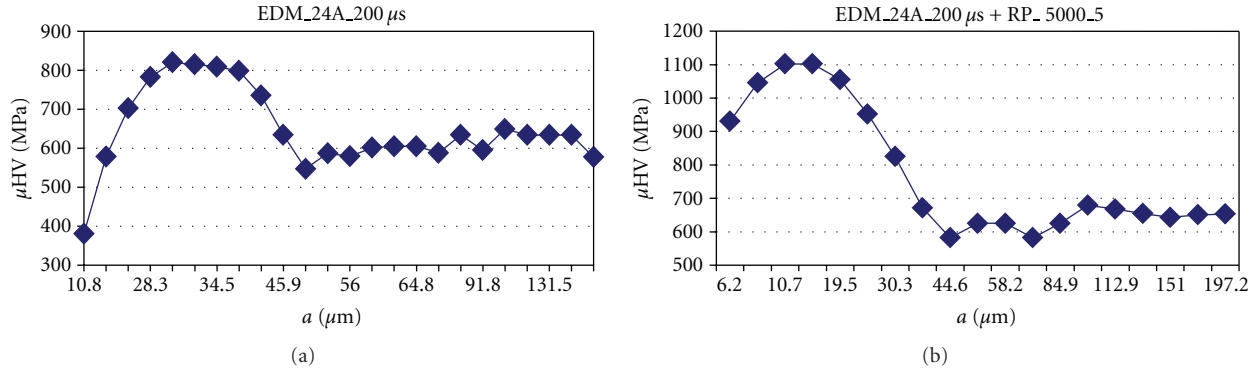

Figure 7: Microhardness distribution in surface layer for EDM $U = 120$ (V), $I = 24$ (A), Ti = 200 (μs), and machined by the EDM and roto-peen $n = 5000$ (rev/min), $t = 5$ (min).

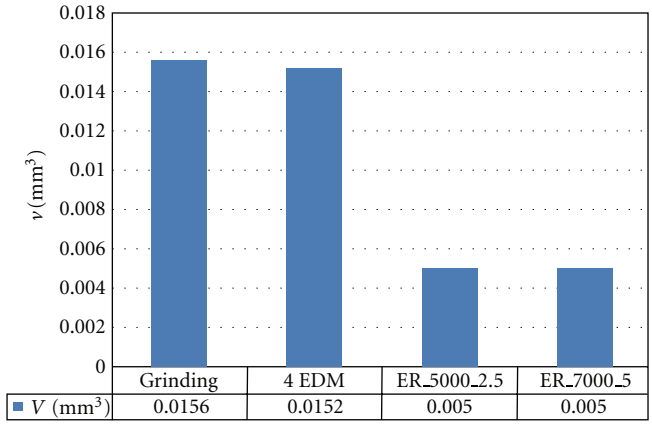

Figure 8: Specification of the resulting resistance to abrasive wear for friction with lubrication of the samples of tool steel NC10 machined by grinding and by the EDM: $U = 80$ (V), $I = 48$ (A), Ti = 400 (μs), and EDM + roto-peen: $n = 5000$ (rev/min), $t = 2.5$ (min), and $n = 7000$ (obr/min), $t = 5$ (min).

specimen which is subjected to friction contact with special antispecimen of ring-like shape made of cemented carbide.

The cold-work superficial treatment can function as a factor both increasing and diminishing abrasive wear of the examined specimens depending on how friction is applied [13].

In the case of lubrication-free friction (specimen immersion in potassium dichromate solution), resistance to wear can be lower because adhesive wear is dominant and the surface is likely to be subjected to adhesive blockade with inner energy increase.

In the case of lubrication contact accompanying abrasive wear process, the hardness increase resulting from the cold-work superficial treatment is likely to contribute to higher abrasive wear resistance.

The test has been repeated three times for each specimen and the average measurement value has been calculated. The experimental investigation for examining the influence of the combined EDM + roto-peen machining on resistance to abrasive wear has been carried out for hardened specimen of tool steel NC10 for the following surfaces: ground surfaces, surfaces subjected to the EDM using various parameters (surfaces featuring various layer properties have been investigated), surfaces subjected to the EDM, and then to the roto-peen treatment under various process parameters (time, rotary speed).

The experimental investigation has been carried out under two different ways of experimental procedures: without lubrication, in potassium dichromate solution and for rotational speed $n = 3000$ (rev/min) and then with lubrication in mixed solution of one part of kerosene and three parts of machine oil. The increase of resistance to abrasive wear when compared to the ground specimen is noticeable regardless of the EDM parameters. Resistance to abrasive wear shows a decrease for the EDM-ed specimens when the EDM parameters are elevated. The roto-peen treatment application after the EDM cause increase in wear resistance for friction in potassium dichromate solution.

The diagram presenting resistance to abrasive wear for friction with lubrication has been shown in Figure 8 for the specimen of tool steel, for various machining variants.

Results of investigating resistance to abrasive wear in lubrication friction by the Skoda-Savin method demonstrate considerable increase in wear resistance of the specimens subjected to subsequent EDM and roto-peen machining

when compared to the ground or EDM-ed specimens (Figure 8).

Fatigue resistance has been investigated for the flat specimens made of heat-treated tool steel NC10 (Rockwell scale hardness was 30). The Schenk PWQ-flato fatigue testing machine has been used, for two-side bending, with bending stress $\sigma = 300 \div 450$ MPa.

Fatigue resistance experiments were limited to general recognition and they were carried out with limited number of variants for specimens machined by the EDM and the EDM+ roto peen for various machining parameters. The specimens after the EDM process carried out for specific parameters have been adopted as a reference condition.

The specimens machined by the EDM and then by the roto-peen at parameters $n = 5000$ (rev/min), $t = 2.5$ (min) and stress $\sigma = 300$ MPa can stand 1 000 000 cycles and for higher stress $\sigma = 350$ MPa they can stand 111 000 ÷ 150 000 cycles. Specimens machined by the roto-peen at parameters $n = 7000$ (rev/min), $t = 2.5$ (min), and stress $\sigma = 350$ MPa or $\sigma = 400$ MPa can stand 1 000 000 cycles while for higher stress $\sigma = 450$ MPa they can stand 107 000 cycles.

One can conclude that if the resistance of the specimens machined by the EDM for stress 350 MPA amounting to over 100 000 cycles and those machined by the EDM and then the roto-peen showed the resistance 470 000 ÷ 1000 000 cycles, the fatigue resistance after the EDM + roto-peen machining is five to ten times higher for the same stress level. The fatigue strength analysis for the specimens subjected to the EDM and EDM + roto-peen at stress 150 MPa showed that the specimens machined by the EDM show similar resistance for stress $\sigma = 150$ MPa that the specimens machined by the EDM and then by the roto-peen for stress $\sigma = 450$ MPa.

The results obtained show that the roto-peen machining applied after the EDM yields the similar effect as much more intensive shot peening applied after the EDM, described in the available bibliography [12, 14].

3. The Investigation of the EDA and the Roto-Peen Influence on Surface Layer Properties and Selected Performance Properties

The investigation of the EDA parameters on surface layer properties and on the selected performance properties has been carried out for the specimens of hardened constructional steel C45. The experiments have been performed using monolithic shape electrodes made of the following materials: alloy steel 1H18N9, tungsten and tungsten carbide. The assessment included the influence of electrical discharge alloying on surface layer properties. The amperage I within the range of 16–48 A and pulse duration time within 25 do 3200 μs were set as independent variables while constant voltage U = 160 V was used as a fixed parameter. The machining took place in the presence of a typical industrial fluid—cosmetic kerosene. The metallographic structure of surface layer after the EDA is presented in Figure 9.

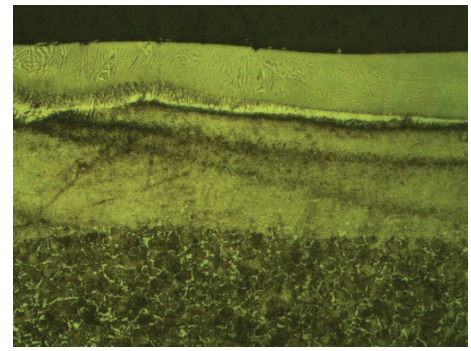

Figure 9: The image of the metallographic structure of surface layer after the EDA: $U = 200$ (V), $I = 32$ (A), Ti = 3200 (μs) (x 250).

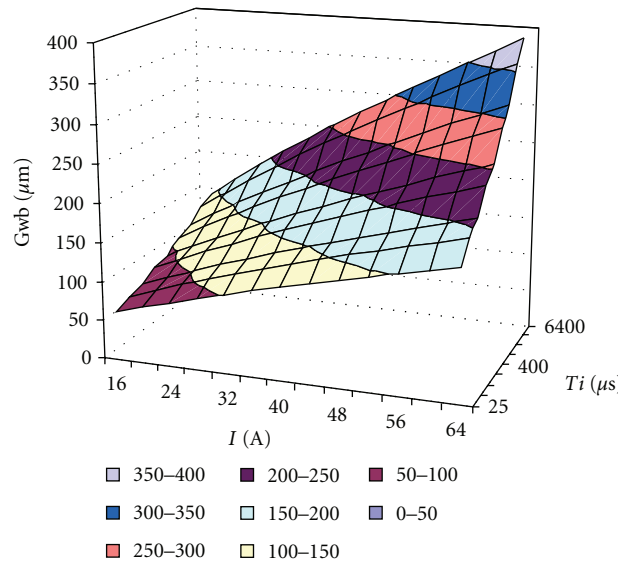

Figure 10: Dependence of the alloyed layer depth on the adopted machining parameters.

The selection of the roto-peen parameters insured various strain hardening depths (which are at least equal to the depth of the remelted layer) and various stress level in surface layer, depth of which should be higher than the depth of stress accumulation in surface layer after the EDA and EDM.

The selection of superficial cold work treatment—the roto-peen should be particularly closely watched [14, 16]. Overly intensive machining, both as to the rotational speed and its duration results in destruction of the remelted layer, microcracking and the layer exfoliation while insufficient parameters do not assure proper surface layer depth [4]. After the preliminary investigations, the range of parameters ensuring good machining results has been determined. Rotational tool speed has been set on a level of $n = 4100$ (rev/min) (maximum allowable speed ensuring that cracks and exfoliation of the alloyed layer would not take place). The times of machining were $t_1 = 75$ (s) and $t_2 = 150$ (s) (area $s = 20$ mm^2).

It is assumed that the surfaces to be alloyed had been subjected to the electrodischarge machining on the same machine tool.

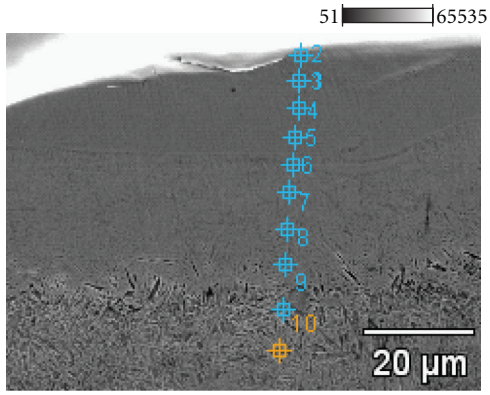

Figure 11: SEM surface layer image after the alloying with the electrode of alloy steel 1H18N9 (I = 32 A, Ti = 25 μs); measuring points (Table 2) have been marked.

Table 2: Specification of the chemical composition investigation results for the surface layer after the alloy steel 1H18N9 electrode alloying; pulse current I = 32 (A), pulse Ti = 25 (μs), electrode material: 1H18N9.

18L	Si-K	Cr-K	Mn-K	Ni-K
*pt*1	0.39	5.91	1.09	2.64
*pt*2	0.35	5.47	1.38	2.60
*pt*3	0.37	3.59	1.14	2.02
*pt*4	0.33	4.85	1.33	1.40
*pt*5	0.38	0.50	0.92	0.00
*pt*6	0.25	0.38	0.51	0.16
*pt*7	0.28	0.29	0.75	0.15
*pt*8	0.42	0.09	1.20	0.44
*pt*9	0.36	0.24	0.63	0.53
*pt*10	0.35	0.19	1.05	0.04

Consequently, the investigation does include eight experiments: two EDM variants, two EDA variants, and two roto-peen variants.

The obtained investigation results enable preliminary assessment of the EDA and EDA + roto-peen and determination of its advisability while having known performance requirements of machine parts in mind.

The obtained average values of the remelted surface layer in the EDA process amount from 30 μm for I = 32 (A), Ti = 25 (μs) to 100 μm for I = 48 (A), Ti = 1600 (μs). The analysis of the obtained results indicate intensive growth of the remelted layer with the pulse amperage increase (Figure 10).

The analysis of chemical composition included the alloyed layer but also the heat-affected zone. It has been conducted in vacuum along the direction which is perpendicular to the specimen surface and taken down the surface layer depth. The analysis show that the alloying process employing the electrode 1H18N9 steel gave the remelted layer depth of about 100 μm with high content of alloying elements where the weight shares of the alloyed layers are following: chromium Cr: 6.7%, nickel Ni: 2.8% at the

Table 3: Specification of the chemical composition investigation results for the surface layer after the tungsten electrode alloying. Pulse current I = 32 (A), pulse Ti = 25 (μs), electrode material: tungsten.

26L	Si-K	Mn-K	W-L
*pt*1	1.52	0.46	33.81
*pt*2	1.02	0.69	28.38
*pt*3	1.19	0.49	17.10
*pt*4	1.08	0.10	31.06
*pt*5	0.11	0.44	1.37
*pt*6	0.27	0.95	0.00
*pt*7	0.25	0.69	0.00
*pt*8	0.27	0.64	0.33
*pt*9	0.21	0.77	0.00

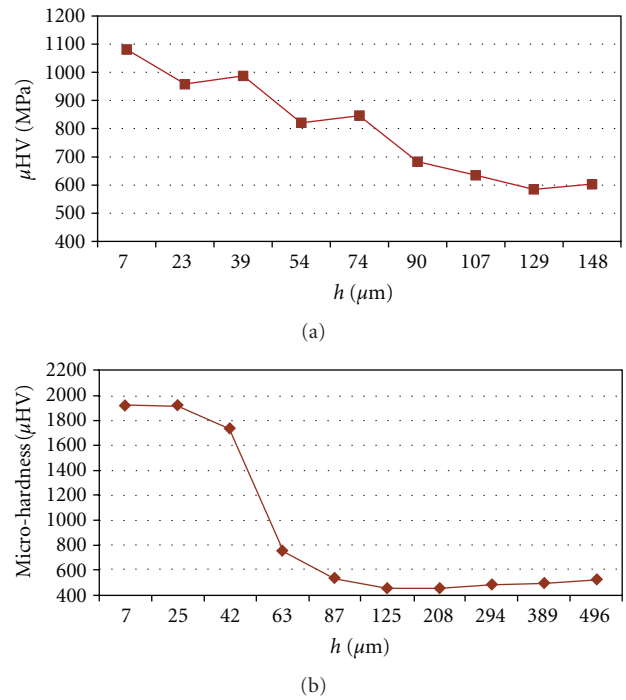

Figure 12: (a) Microhardness versus the distance from the edge for the specimen machined by the tungsten electrode at the following parameters. (a) EDA I = 24 (A), Ti = 400 (μs), (b) EDA I = 24 (A). Ti = 400 (μs) and then the roto-peen n = 4100 (rev/min), t = 75 (s).

following alloying parameters: pulse amperage: 48 A, pulse duration: 1600 μs (Table 2; Figure 11). For the electrodes with different materials like tungsten and tungsten carbide, saturation of surface layer with the elements coming form the tool electrode is also visible (Table 3). For the alloying process carried out with tungsten electrode at the following parameters: pulse amperage 64 A, pulse time 400 μs, the weight share in surface layer is 6% for tungsten on the average and it is higher amounting respectively up to 33% tungsten for the experiments conducted at elevated pulse amperage 48 A and pulse duration: 1600 μs. Maximum volume share

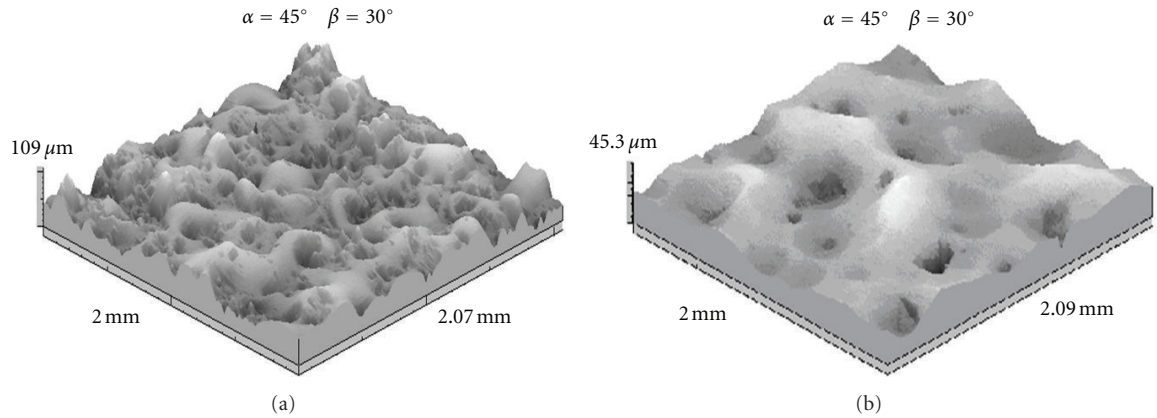

Figure 13: Stereometric image of the surface subjected to the: (a) EDA: 1H18N9 electrode, $I = 24$ (A), Ti = 400 (μs), $U = 200$ (V), (c) EDA + roto peen $n = 4100$ (obr/min), $t = 75$ (s).

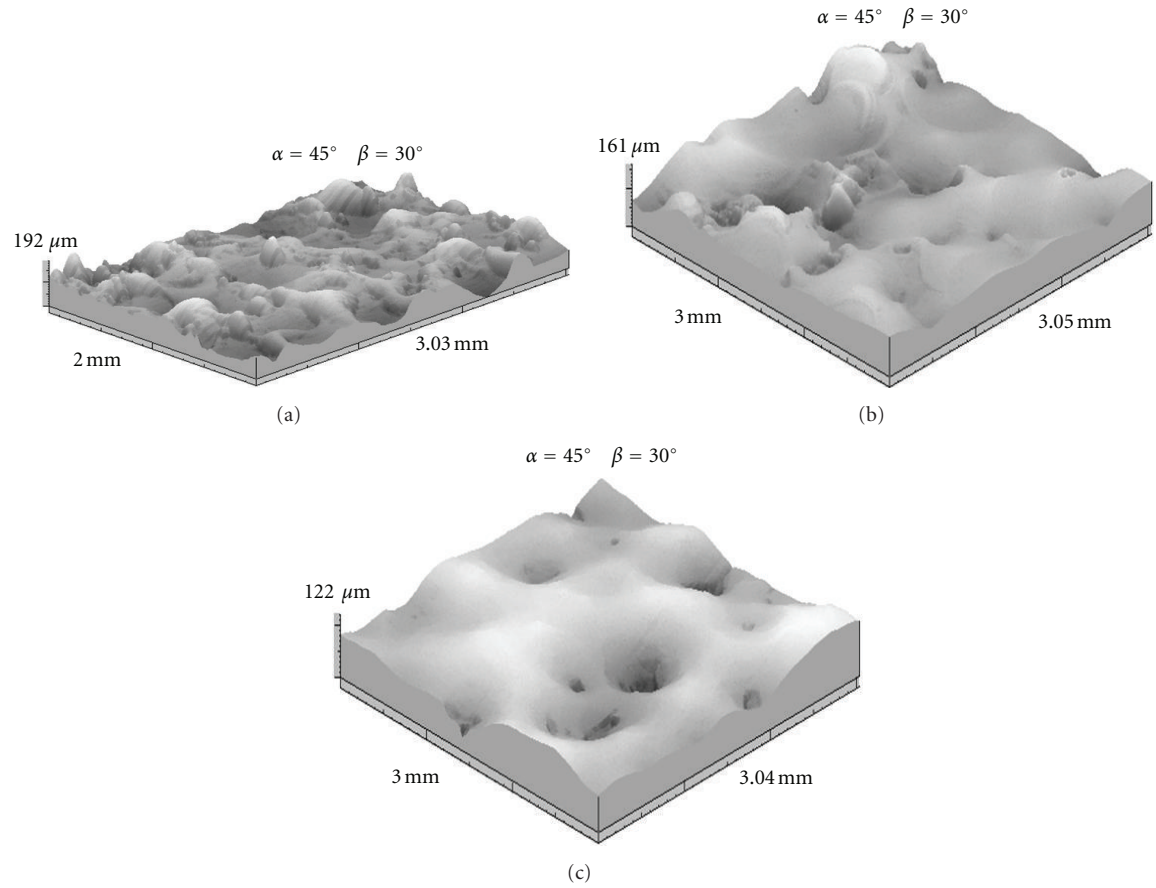

Figure 14: Stereometric image of the surface subjected to the: (a) EDM: cooper electrode, $I = 32$ (A), Ti = 800 (μs); (b) EDA: 1H18N9 electrode, $I = 32$ (A), Ti = 3200 (μs); (c) EDA + roto peen; $n = 4100$ (rev/min), $t = 75$ (s).

of anode material in the superficial layer of the alloyed part amounted form 20% to 30%.

The points for which the chemical composition has been determined, are shown in Figure 11 with surface layer visible in the background.

In the typical microhardness pattern being a function of distance from the edge, one can see the increase from 600 μHV in the core up to 800–1100 μHV nearby the specimen surface (Figure 12). Microhardness is usually highest at the surface and it gradually lowers with the depth. Micro-hardness of the heat-affected zone is lower than the micro-hardness of the remelted layer but it is higher that the micro-hardness of the material core.

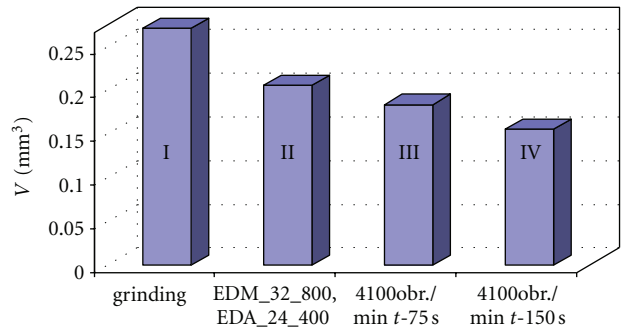

Figure 15: Comparative results. Investigation of abrasive wear resistance measured with Skoda-Savin method: (I) samples of steel 45 machined by grinding, (II) EDM $U = 180$ (V), $I = 32$ (A), Ti = 800 (μs) and EDA: $U = 200$ (V), $I = 24$ (A), Ti = 400 (μs); (III, IV) EDM, EDA and with roto peen: $n = 4100$ (rev/min) for the time of: $t = 75$ (s) (III); $t = 150$ (s) (IV). (lubrication free conditions–specimen immersion in potassium dichromate).

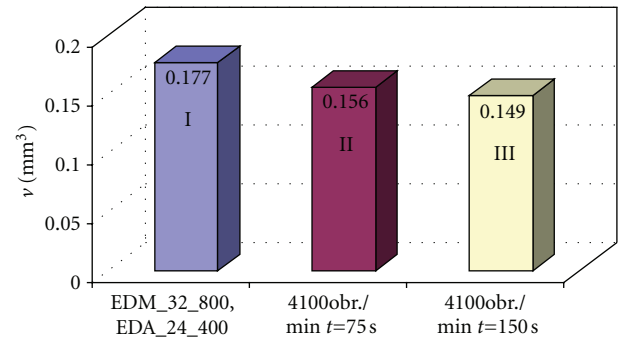

Figure 16: Comparative results. Investigation of abrasive wear resistance measured with Skoda-Savin method: (I) samples of steel 45 machined by grinding, (II) EDM—$U = 180$ V, $I = 32$ A, Ti = 800 μs and EDA: $U = 200$ V, $I = 24$ A, Ti = 400 μs; (III, IV) EDM, EDA and with roto peen: $n = 4100$ rev/min for the time of: $t = 75$ s (III); $t = 150$ s (IV). (Lubrication conditions—kerosene and machine oil solution −1 : 3).

The geometrical microstructure investigation showed that application of the roto-peen after the EDA results in twofold decrease of the roughness, for example Ra goes down from 8 to 4 μm. The obtained micro-structure is of highly favorable pattern (similar to one obtained after the EDM + roto-peen) of flat summits and indents remaining after the EDM (Figures 13 and 14).

The investigation of performance properties resulting from the EDA and the combined EDM + roto-peen included resistance to abrasive wear and fatigue strength. Figures 15 and 16 show dependence of the observed wear examined by the Skoda-savin method for the lubricated machined samples on the applied manufacturing variants. The performed analysis shows that the EDA application results in considerable resistance to wear when compared to ground surfaces and additional application of the roto-peen after the EDA causes an extra increase in abrasive wear resistance.

Preliminary investigation of fatigue resistance of the specimens machined by the EDA + roto-peen, carried out in identical environment like the samples after the EDM showed that the application of the roto-peen machining after the EDA, gives the similar result of fatigue strength increase and durability to the one obtained when applying the roto-peen after the EDM.

4. Conclusions

The application of the superficial cold-work treatment represented by the roto-peen machining applied after the EDM and the EDA contributes to considerable lowering of roughness height, (50–70%), reduction in surface layer microcrack and discontinuity number as well as elevation of surface layer microhardness by 300 μHV in the case of the EDM and 700 μHV for the EDA.

The roto-peen application results in considerable increase of abrasive wear resistance, 3-fold for the EDM, and 40% for the EDA.

The roto-peen application is relatively cheap and practically simple operation which can be realized with the universally available equipment; both the EDA and the roto-peen machining are particularly dedicated to the treatment of small surface areas or the selected portions of large parts.

The EDA and roto-peen machining can be applied for improving performance properties of machine and tool parts which are the most exposed to wear.

References

[1] J. P. Kurth, J. Van Humbeeck, and L. Stevens, "Micro structural investigation and metallographic analysis of the white layer of a surface machined by Electro Discharge Machining," in *Proceedings of the 11th International Symposium on Emergency Management (ISEM '95)*, pp. 849–862, Lausanne, Switzerland, 1995.

[2] M. Siwczyk, *Electrical Discharge Machining Obróbka Elektroerozyjna*, WNT, Warsaw, Poland, 1981.

[3] B. Nowicki, R. Pierzynowski, and S. Spadło, "Comperative investigation into the brush electrodischarge alloying with the electrodes of alloy steel and tungsten," *International Journal for Manufacturing Science and Technology*, vol. 4, no. 1, pp. 44–54, 2004.

[4] Collective work Electrical discharge allying of metal surfaces, Elektroiskrowoe legirowanie metaliceskich powerchnostej, Akadamia Nauk USSR, 1976.

[5] L. C. Lim, L. C. Lee, Y. S. Wong, and H. H. Lu, "Solidification microstructure of electrodischarge machined surfaces of tool steels," *Materials Science and Technology*, vol. 7, no. 3, pp. 239–248, 1991.

[6] J. A. McGeough and H. Rasmussen, "A macroscopic model of electro-discharge machining," *International Journal of Machine Tool Design and Research*, vol. 22, no. 4, pp. 333–339, 1982.

[7] A. Dmowska, B. Nowicki, and A. Podolak-Lejtas, "A new method of investigating crater and flash made by individual discharge using scanning profilometers," *Metrology and Properties of Engineering Surfaces, Rzeszów*, pp. 139–145, 2011.

[8] B. Ekmekci, "Residual stresses and white layer in electric discharge machining (EDM)," *Applied Surface Science*, vol. 253, no. 23, pp. 9234–9240, 2007.

[9] H. T. Lee and T. Y. Tai, "Relationship between EDM parameters and surface crack formation," *Journal of Materials Processing Technology*, vol. 142, no. 3, pp. 676–683, 2003.
[10] P. G. Bailey, "Manual peening with the rotary flap process," in *Proceedings of the 7th International conference on shot peening, Poland*, pp. 405–414, Warsaw, Poland, 1999.
[11] M. Drozd, A. Fedorov, and J. Cidjakin, "Rascet głubiny rosprostranienia plasticeskih deformatcji," *Westnik Mashinostroenija*, no. 1, pp. 132–137, 1972.
[12] A. Nakonieczny, T. Żółciak, and G. Monka, "Effects of shot peening on process of carburization and selected strength properties of steel 18 HGT," in *Proceedings of the International Conference on Shot Peening*, pp. 135–144, Warsaw, Poland, 1999.
[13] W. Przybylski, *Burnishing Technology Technologia Obróbki Nagniataniem*, Wydawnictwo Naukowo-Techniczne, Warsaw, Poland, 1987.
[14] Y. C. Lin, B. H. Yan, and F. Y. Huang, "Surface improvement using a combination of electrical discharge machining with ball burnish machining based on the taguchi method," *International Journal of Advanced Manufacturing Technology*, vol. 18, no. 9, pp. 673–682, 2001.
[15] B. Nowicki and A. Podolak-Lejtas, "Investigations of the effect of combined EDM machining with burnishing process on the conditio of the surface layer," *Advances in Manufacturing Science and Technology*, vol. 32, no. 8, 2008.
[16] American National Standard for Surface Integrity B 211.1.1986.